Available online at www.sciencedirect.com
ScienceDirect
Journal of Power Sources 165 (2007) 635–639
JOURNAL OF POWER SOURCES
www.elsevier.com/locate/jpowsour

Short communication

# Improved high power Li-ion batteries with $Li_2RuO_3$ addition: A fast charging and fast cycling study

Arnold M. Stux *, Karen E. Swider-Lyons

*Code 6113, Naval Research Laboratory, Washington, DC 20375, USA*

Available online 22 November 2006

**Abstract**

The high-rate charging and cycling of Li-ion batteries is improved by blending $Li_2RuO_3$ into $LiCoO_2$ cathodes in cells with $Li_4Ti_5O_{12}$ anodes. The cathode-limited cells have greater discharge capacities when $Li_2RuO_3$-containing cathodes are recharged up to 2*C* rates. The $Li_4Ti_5O_{12}/Li_2RuO_3 + LiCoO_2$ cells also show capacity increases over initial cycles and minimal capacity decay when cycled at a 2*C* rate over 50 cycles. These benefits are attributed to the reduced cell impedance of the $Li_2RuO_3$-containing cathodes.
Published by Elsevier B.V.

*Keywords:* Rapid recharging; Microbatteries; Li-ion batteries; $Li_2RuO_3$; $Li_4Ti_5O_{12}$; High rate

## 1. Introduction

Miniaturized rechargeable lithium-ion batteries are attractive power sources for autonomous microdevices because of their high specific energy, long cycle life, and minimal electronic disruption to microelectronic systems. These devices typically require high energy and high power, plus capability for rapid recharging. High power and rapid recharging are a challenge because the capacities of Li-ion cells decrease with increasing discharge and charge rates. We have previously shown that the specific power and energy at high cycling rates, such as 2*C*, is improved by the addition of $Li_2RuO_3$ to $LiCoO_2$ in the cathodes of Li-ion batteries with carbonaceous anodes [1]. Blended cathodes of $LiCoO_2$ and $Li_2RuO_3$ were particularly effective; combining these insertion materials so that they were electrically in parallel resulted in reduced cell impedance and low IR losses in the cells.

$Li_2RuO_3$ is a stable $Li^+$ insertion compound with high electronic and Li-ion conductivity and high volumetric capacity [2–4]. Physical mixing of $Li_2RuO_3$ and another $Li^+$ insertion material is a favorable approach because it utilizes both the low resistivity of $Li_2RuO_3$ and the reversibility of $Li^+$ insertion and de-insertion. In pure $Li_2RuO_3$ electrodes, the $Ru^{5+/4+}$ redox couple permits facile $Li^+$ liberation. Approximately one mole of $Li^+$ is extracted per mole $Li_2RuO_3$ within common testing voltage ranges. $Li_2RuO_3$ has two voltage plateaus at both 3.6 and 3.4 V, which had been correlated to two distinct biphasic regimes [2]. The 3.6 V plateau corresponds to compositions of $0.7 < x < 1.0$ in $Li_{2-x}RuO_3$.

One approach to improving the charging rate capability of Li-ion batteries is to use $Li_4Ti_5O_{12}$ as the active material in the anode [5]. The reduction potential of $Li_4Ti_5O_{12}$ is 1.5 V versus $Li^+/Li$, so it does not form a resistive solid electrolyte interphase (SEI) layer, which impedes charging and discharge rates [5,6]. The 1.5 V potential also eliminates any risk of Li metal plating during fast charging. $Li_4Ti_5O_{12}$ is often selected in conjunction with experimental ionic liquid-based electrolytes in order to avoid cathodic decomposition of the electrolyte solvent during cycling [7,8]. $Li_4Ti_5O_{12}$ also exhibits no dimensional changes with $Li^+$ intercalation, and is available in nano-sized particles. Its fine particles allow diffusion of $Li^+$ over small distances in and out of the host lattice structure [6,9]. Selection of $LiFePO_4$ cathodes with $Li_4Ti_5O_{12}$ anodes has been recently promoted because $LiFePO_4$ is environmentally friendly and inexpensive. One criticism of the $Li_4Ti_5O_{12}/LiFePO_4$ cells is that they have low voltage—about 2.0 V. Moreover, the conductivity of $LiFePO_4$ is poor, although some measures have been taken to increase the conductivity with dispersion of carbon [10]. Higher cell voltages of 2.4 V are obtained when the $Li_4Ti_5O_{12}$ is coupled with $LiCoO_2$ [11], a somewhat expensive but well-performing and commercially successful Li-ion battery cathode material. For microdevices,

* Corresponding author. Tel.: +1 202 404 3340; fax: +1 202 404 8119.
*E-mail address:* arnold.stux@nrl.navy.mil (A.M. Stux).

0378-7753/$ – see front matter. Published by Elsevier B.V.
doi:10.1016/j.jpowsour.2006.10.032

high power performance can be more important than materials cost.

This investigation shows how engineering the cathode formulation can improve the charging rate capability of Li-ion batteries beyond simple use of $Li_4Ti_5O_{12}$ anodes. Detailed rate studies are used to demonstrate the effects of the addition of $Li_2RuO_3$ to $LiCoO_2$-based cathodes. Our method is to charge cells at different rates but to discharge them at the slower rate of *C*/5. Each discharge profile is affected by its preceding recharge rate. We present an approach that involves cathode-limited cells with $Li_4Ti_5O_{12}$ anodes, maintains nearly 2.4 V plateaus, and further improves recharge capability. Specifically, we compare cells with and without $Li_2RuO_3$ in the cathode for both rapid recharge up to 2*C* and rapid cycling at 2*C* in cathode-limited Li-ion cells.

## 2. Experimental

### 2.1. Materials

$Li_2RuO_3$ was synthesized by mixing commercially available powders of $RuO_2$ and $Li_2CO_3$ following previously described procedures [2,3]. Briefly, hydrous $RuO_2$ (Alfa Aesar) was dried at 400 °C for 18 h to remove structural water. Afterwards, the $RuO_2$ was ground together with an equimolar amount of $Li_2CO_3$ (Alfa Aesar), pelletized, and sintered in air at 950 °C for 24 h. The pellets were then pulverized using an agate mortar and pestle and sieved to approximately 30 μm. Commercially available $LiCoO_2$ was used as the standard cathode active material.

Cathodes were prepared using $LiCoO_2$ or a 60:40 (w/w) mixture of $LiCoO_2$ and $Li_2RuO_3$, respectively, as the active $Li^+$ insertion constituent of the slurry. Anodes of $Li_4Ti_5O_{12}$ (NEI, less than 500 nm particles) were similarly prepared.

### 2.2. Electrode fabrication

The active materials were formulated into slurries using previously developed recipes [12]. The cathode slurries were a mixture of approximately 91 wt% active cathode material, 2% Super P carbon (Ensaco), 4% KS6 carbon (Timcal), and 3% polyvinylidene fluoride (PVDF, Atofina). The carbon additives were ground with the active material or stirred in the slurry. The PVDF was dissolved separately in 1-methyl-2-pyrrolidone (NMP, Aldrich) and then combined with the active material/carbon powders to make viscous ink for efficient deposition. For the Li-ion cells, anode slurries were prepared from 87% $Li_4Ti_5O_{12}$, 1.5% Super P carbon, and 8.5% PVDF dissolved in NMP. An ink was prepared from 10% Super P carbon and 90% PVDF in NMP to serve as a conductive coating and adhesion layer to the current collectors.

The slurries were deposited on current collectors of aluminum and copper foils (All-Foils, Inc.) approximately 4 mm × 4 mm in area. The Al and Cu foils were pre-treated by etching with 1 M potassium hydroxide and 1 M nitric acid solutions, respectively, followed by rinsing with water and then acetone. A layer of the conductive carbon ink was then added to their surfaces. The conductive coating/adhesion layer was dried on a hot plate at the lowest heat setting for approximately 1 min in order to obtain a homogeneous film. The anode and cathode slurries were then deposited on the carbon-coated Cu and Al foils, respectively. The electrodes were subsequently dried again on the hotplate, and then vacuum-dried overnight 90–95 °C before transferring to an argon-filled glove box. The electrodes were not calendered or pressed. Cells were constructed with weight ratios of positive to negative active materials so that the capacity was limited by the active material in the cathode. The weight of the active materials was 0.6–0.8 mg for the cathodes used with Li anodes. The weights of the active materials in the cathodes were 0.3–0.5 mg and those of the $Li_4Ti_5O_{12}$ in the anodes were 0.4–0.6 mg. For Li test cells, metallic Li foil was fixed to the Cu foil to form the anode, whereby the Li could be used as both a counter and a reference electrode.

### 2.3. Electrochemical investigation

The $LiCoO_2$ and $Li_2RuO_3$ cathode blends were evaluated in packaged Li-ion cells at room temperature both using metallic Li and $Li_4Ti_5O_{12}$. The electrolyte was 1 M $LiPF_6$ in a mixture of carbonates containing ethylene carbonate, propylene carbonate, ethyl methyl carbonate, and diethyl carbonate. The Li-ion microbatteries, or small packaged cells, were assembled using the procedures described previously [12]. A microporous polymer film (Celgard 2730) was used as a separator and sandwiched between the $LiCoO_2$/carbon/aluminum and $Li_4Ti_5O_{12}$/carbon/copper electrodes. The cathode/separator/anode sandwiches were first held together by impulse sealing them in a transparent polymer bag (Saranex SX 23-P), followed by sealing in another pouch of a tri-layer polyethylene–aluminum–polyester. During the sealing process, small holes were left in the polymer seals to allow electrolyte injection. After the battery was filled with the electrolyte, the pouch was fully sealed. With this packaging process, the Li-ion batteries were protected from ambient air and gently held together with no additional pressure on the electrodes.

The electrochemical testing of Li-ion cells was conducted using a battery tester (Maccor 2300) set to cut-off voltages. For cells with the $Li_4Ti_5O_{12}$ anodes, the cut-off voltages were 1.1 and 2.75 V. For cells with the Li anodes, the cut-off voltages were 2.5 and 4.15 V. Cells were cycled at *C*/5, charged at various rates with intermittent *C*/5 discharge, and then cycled at 2*C*. The charge rates with intermittent *C*/5 discharges were *C*/5, *C*/3, *C*/2, *C*, 3*C*/2, and 2*C* corresponding to constant currents ranging from 0.15 to 1.5 mA $cm^2$. For the blends, appropriate currents were determined by normalizing the weighted averages of the single-component specific capacities of discharge at *C*/5 rates. The test current densities were adjusted according to the total mass of active material(s), and the specific capacities initially measured for $LiCoO_2$ (122 mAh $g^{-1}$) and $Li_2RuO_3$ (140 mAh $g^{-1}$).

## 3. Results

### 3.1. Fast charging

Fig. 1 shows the charge and discharge profiles of the $Li_4Ti_5O_{12}$/$LiCoO_2$ cells. In this figure, "time zero" begins after

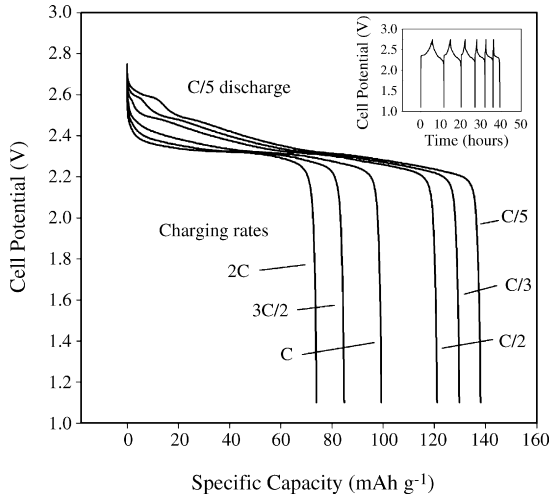


Fig. 1. Discharge profiles of $Li_4Ti_5O_{12}/LiCoO_2$ cells discharged at *C*/5 but preceded by indicated charge rates of *C*/5, *C*/3, *C*/2, *C*, 3*C*/2, and 2*C* rates but with *C*/5 discharge rates. The inset shows the cycling profile of $Li_4Ti_5O_{12}/LiCoO_2$ with successive charging of *C*/5, *C*/3, *C*/2, *C*, 3*C*/2, and 2*C* rates but with *C*/5 discharge rates.

the fifth *C*/5 cycle and at the beginning of the rate study. The $Li_4Ti_5O_{12}/Li_2RuO_3 + LiCoO_2$ cell in Fig. 2 has additional lower voltage plateaus in the discharge profiles near 2.0 V, corresponding to insertion and de-insertion of $Li^+$ in and out of $Li_2RuO_3$. Visual comparison of the figures reveals that the *C*/5 discharge times of the $Li_4Ti_5O_{12}/LiCoO_2$ cells decrease more with increasing charge rates than those of the $Li_4Ti_5O_{12}/Li_2RuO_3 + LiCoO_2$ cell.

The *C*/5 discharge profiles for the same $Li_4Ti_5O_{12}/LiCoO_2$ and $Li_4Ti_5O_{12}/Li_2RuO_3 + LiCoO_2$ cells in Figs. 1 and 2 are insets and show how varying the recharge rates from *C*/5 to 2*C* between 1.1 and 2.75 V affects the capacity of the *C*/5 discharge. For both types of cells, the voltage plateaus are flat at potentials of 2.4 V with respect to the $Li/Li^+$ potential when $Li_4Ti_5O_{12}$

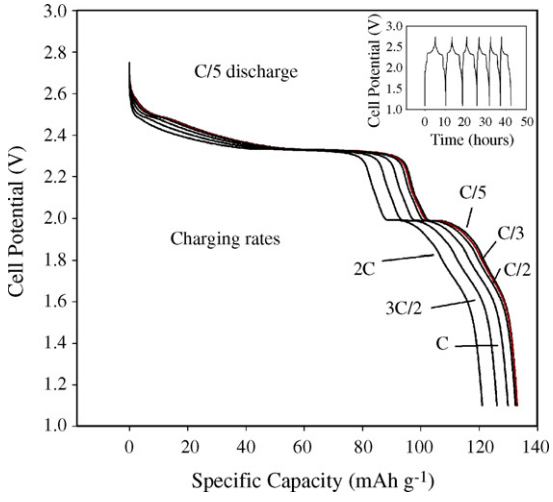


Fig. 2. Discharge profiles of $Li_4Ti_5O_{12}/LiCoO_2 + Li_2RuO_3$ cells discharged at *C*/5 but preceded by indicated charge rates of *C*/5, *C*/3, *C*/2, *C*, 3*C*/2, and 2*C* rates but with *C*/5 discharge rates. The inset shows the cycling profile of $Li_4Ti_5O_{12}/LiCoO_2 + Li_2RuO_3$ cells with successive charging of *C*/5, *C*/3, *C*/2, *C*, 3*C*/2, and 2*C* rates but with *C*/5 discharge rates.

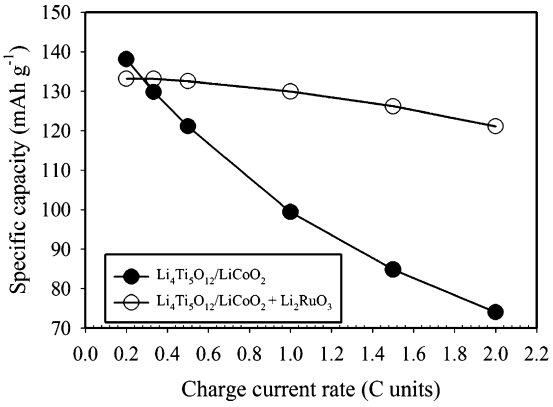


Fig. 3. Comparison of *C*/5 discharge capacities of $Li_4Ti_5O_{12}/LiCoO_2$ and $Li_4Ti_5O_{12}/LiCoO_2 + Li_2RuO_3$ cells as a function of charge rate.

is used as the anode. The *C*/5 discharge capacities following *C*/5, *C*/3, and *C*/2 charging are 138, 129, and 121 mAh $g^{-1}$ for the $Li_4Ti_5O_{12}/LiCoO_2$ cell but are all 133 mAh $g^{-1}$ for the $Li_4Ti_5O_{12}/Li_2RuO_3 + LiCoO_2$ cell. The decrease in the *C*/5 discharge capacity, with the testing protocol described in Section 2.3, is less for the $Li_4Ti_5O_{12}/Li_2RuO_3 + LiCoO_2$ cells than for the $Li_4Ti_5O_{12}/LiCoO_2$ cells. For the pure $LiCoO_2$ cathode, despite starting at 2.75 V, the initial voltages of the discharge curves decrease with an increase of the preceding charge rate, indicating initial drop to a lower state of charge. The $Li_4Ti_5O_{12}/Li_2RuO_3 + LiCoO_2$ cells maintain flat discharge curves even with increasing recharge rates, indicating little ohmic loss.

Fig. 3 summarizes the data in Figs. 1 and 2 and demonstrates that the specific capacity of the $Li_4Ti_5O_{12}/LiCoO_2$ cells discharged at a *C*/5 rate decreases more with charging rate than the $Li_4Ti_5O_{12}/Li_2RuO_3 + LiCoO_2$ cells.

Fig. 4 shows discharge profiles for cells with metallic Li anodes and $Li_2RuO_3 + LiCoO_2$ cathodes. The shapes of the curves are similar to those of the $Li_4Ti_5O_{12}/Li_2RuO_3 + LiCoO_2$ cells. The plateaus corresponding to insertion and de-insertion of $Li^+$ in and out of $Li_2RuO_3$ are prominent in these Li-cells and show no decrease in these cycles, while the capacity associated

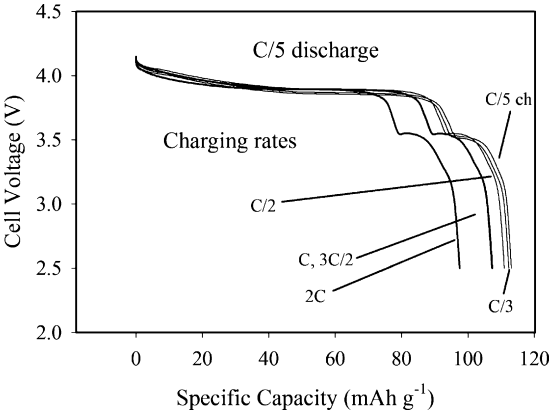


Fig. 4. Discharge profiles of lithium cells, comprised of $LiCoO_2$:$Li_2RuO_3$ 60:40 (w/w) cathodes and metallic Li anodes, discharged at *C*/5 followed by indicated charge rates.

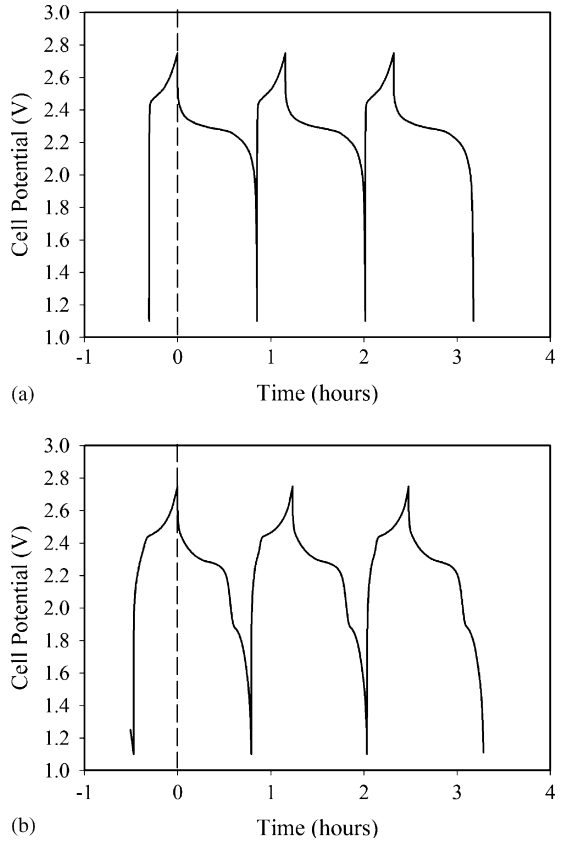


Fig. 5. Cycling profile of (a) $Li_4Ti_5O_{12}/LiCoO_2$ cells and (b) $Li_4Ti_5O_{12}/LiCoO_2 + Li_2RuO_3$ at 2*C* rate.

with $LiCoO_2$ shows marked decrease with increasing recharge rate.

### 3.2. Fast cycling

Fig. 5 shows representative 2*C* charge–discharge cycles of $Li_4Ti_5O_{12}/LiCoO_2$ and $Li_4Ti_5O_{12}/Li_2RuO_3 + LiCoO_2$ cells after completion of the varied rate tests shown in Figs. 1 and 2. The specific capacities increase over the first 12 cycles before levelling off for the $Li_4Ti_5O_{12}/Li_2RuO_3 + LiCoO_2$ cell, whereas fade begins immediately after the first cycle at the 2*C* rate with the $Li_4Ti_5O_{12}/LiCoO_2$ cell. Fig. 6 shows the specific capacities of $Li_4Ti_5O_{12}/Li_2RuO_3 + LiCoO_2$ cells for up to 50 cycles. The inset shows a comparison of the trends in capacities for cells using these two types of cathodes. The fade rate is generally lower for the $Li_4Ti_5O_{12}/Li_2RuO_3 + LiCoO_2$ cells than the $Li_4Ti_5O_{12}/LiCoO_2$ cells. The cells with $Li_2RuO_3$ as one of the active cathode materials have superior cycling durability to those without.

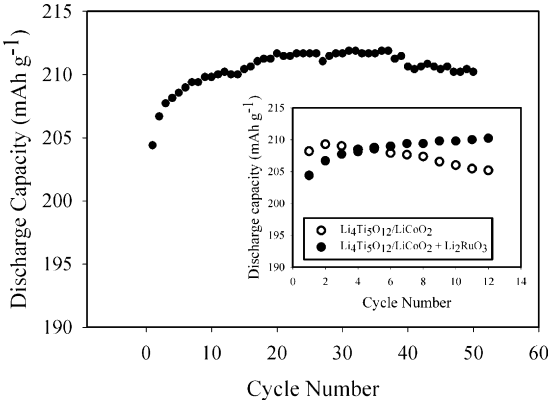


Fig. 6. Discharge capacities of $Li_4Ti_5O_{12}/LiCoO_2 + Li_2RuO_3$ as a function of cycle number. *Inset*: Comparison of initial specific capacities on discharge for cells cycled at 2*C*, both with $Li_4Ti_5O_{12}/LiCoO_2 + Li_2RuO_3$ and $Li_4Ti_5O_{12}/LiCoO_2$ cells.

## 4. Discussion

The addition of $Li_2RuO_3$ to $LiCoO_2$ cathodes enhances the ability for fast charging and fast cycling of Li-ion cells with $Li_4Ti_5O_{12}$ anodes. Generally, the discharge capacities of Li-ion cells decrease with both increasing discharge and recharge rates. This trend is mitigated in the $Li_4Ti_5O_{12}/Li_2RuO_3 + LiCoO_2$ cells because $Li_2RuO_3$ is a low-impedance material, allows fast charging without a deleterious effect to the discharge capacity, and causes the blend to have less polarization. The impedance of cells with electrodes containing $Li_2RuO_3$ as part or all of the active material was shown previously to be lower than cells with pure $LiCoO_2$-based cathodes [1]. $Li_2RuO_3$ improves the electrochemical kinetics of cells with $LiCoO_2$ because $Li_2RuO_3$ has a low resistivity of 10 Ω cm [13]. $Li_2RuO_3$ also promotes the utility of $LiCoO_2$ by virtue of only its conductive properties, creating a more extensive conductive network and enhancing the interparticle electronic conductivity of $LiCoO_2$, as $RuO_2$ does in $V_2O_5$ [14] and $LiMn_2O_4$ [15]. Also, there is extra capacity at 2.0 V with the testing cut-off voltages for the $Li_4Ti_5O_{12}/Li_2RuO_3 + LiCoO_2$ cell, even with the *C*/2 and 2*C* rates, because of the $Li_2RuO_3$.

The $Li_2RuO_3$ additionally enhances electrode utility as evidenced by the increasing specific capacity over the first 12 2*C*-rate cycles for the cell using the cathode blend (Fig. 6). This supports early reports of kinetically fast electrochemical delithiation from $Li_2RuO_3$ [4]. It further suggests cation disorder and movement of Ru to different lattice sites within the $LiRu_2$ layers upon deintercalation of $Li^+$. In situ X-ray diffraction at various states of charge may be needed to probe this further.

Percolation networks also play a role because the effect reported in this study relies on optimization of connectivity. It is likely that adjustments to the materials' particle size, morphology, and their relative concentration (or volume) can be made to further improve the performance of the electrodes. The use of nanoparticles in the cathode blends can also improve the performance as ionic conductivity can increase with decreasing particle size, although the electronic conductivity may decrease [16]. Although $Li_2RuO_3$ is acceptable for applications requiring small amounts of active material, such as microbatteries, its benefit might not be economically viable for large batteries due to the high cost of ruthenium. Nevertheless, lessons can be applied to other low-impedance materials.

## 5. Conclusions

The rate and power capability of Li-ion batteries with $Li_4Ti_5O_{12}$ anodes are increased by blending $Li_2RuO_3$ into the $LiCoO_2$ cathodes. The $Li_2RuO_3$ and $LiCoO_2$ are combined in parallel via a physical mixing or blending of the two $Li^+$ insertion materials. An improvement in capacity is shown during both rapid recharging and fast cycling testing procedures. The $Li_2RuO_3 + LiCoO_2$ cells can be implemented on a small scale with $Li_4Ti_5O_{12}$ for high power 2.4 V cells with no addition to standardized processes other than the preparation of $Li_2RuO_3$.

## Acknowledgments

We would like to acknowledge the Office of Naval Research and DARPA MTO for support of this research.

## References

[1] A.M. Stux, K.E. Swider-Lyons, J. Electrochem. Soc. 152 (2005) A2009–A2016.
[2] H. Kobayashi, R. Kanno, Y. Kamamoto, M. Tabuchi, O. Nakamura, M. Takano, Solid State Ionics 82 (1995) 25–31.
[3] G.J. Moore, C.S. Johnson, M.M. Thackeray, J. Power Sources 119–121 (2003) 216–220.
[4] A.C.W.P. James, J.B. Goodenough, J. Solid State Chem. 76 (1988) 287–294.
[5] A. Du Pasquier, I. Plitz, J. Gural, F. Badway, G.G. Amatucci, J. Power Sources 136 (2004) 160–170.
[6] A. Singhal, G. Skandan, G. Amatucci, F. Badway, N. Ye, A. Manthiram, H. Ye, J.J. Xu, J. Power Sources 129 (2004) 32–44.
[7] T. Sato, T. Maruo, S. Marukane, K. Takagi, J. Power Sources 138 (2004) 253–261.
[8] H. Nakagawa, S. Izuchi, K. Kuwana, Y. Aihara, J. Electrochem. Soc. 150 (2003) A695–A700.
[9] L. Kavan, M. Grätzel, Electrochem. Solid-State Lett. 5 (2002) A39–A42.
[10] N. Ravet, J.B. Goodenough, S. Besner, M. Gauthier, M. Armand, J. Power Sources 97–98 (2001) 503–507.
[11] A.N. Jansen, A.J. Kahaian, K.D. Kepler, P.A. Nelson, K. Amine, D.W. Dees, D.R. Vissers, M.M. Thackeray, J. Power Sources 81–82 (1999) 902–905.
[12] R. Wartena, A.E. Curtright, C.B. Arnold, A. Pique, K.E. Swider-Lyons, J. Power Sources 126 (2004) 193–202.
[13] H. Kobayashi, R. Kanno, Y. Kamamoto, M. Tabuchi, O. Nakamura, M. Takano, Solid State Ionics 86–88 (1996) 859–863.
[14] F. Zhang, S. Passerini, B.B. Owens, W.H. Smyrl, Electrochem. Solid-State Lett. 4 (2001) A221–A223.
[15] M. Carewska, G.B. Appetechi, F. Cardellini, S. Passerini, Solid State Ionics 139 (2001) 211–218.
[16] P. Balaya, H. Li, K. Lorentz, J. Maier, Adv. Funct. Mater. 13 (2003) 621–625.